Current Biology, Vol. 14, 1863–1870, October 26, 2004, ©2004 Elsevier Ltd. All rights reserved. DOI 10.1016/j.cub.2004.09.085

The *Drosophila* Fragile X Gene Negatively Regulates Neuronal Elaboration and Synaptic Differentiation

Luyuan Pan, Yong Q. Zhang, Elvin Woodruff, and Kendal Broadie*
Department of Biological Science
Kennedy Center for Research on Human Development
Vanderbilt University
Nashville, Tennessee 37232

Summary

Fragile X Syndrome (FraX) is the most common form of inherited mental retardation. The disease is caused by the silencing of the *fragile X mental retardation 1* (*fmr1*) gene, which encodes the RNA binding translational regulator FMRP [1–4]. In FraX patients and *fmr1* knockout mice, loss of FMRP causes denser and morphologically altered postsynaptic dendritic spines [5–7]. Previously, we established a *Drosophila* FraX model and showed that dFMRP acts as a negative translational regulator of Futsch/MAP1B and negatively regulates synaptic branching and structural elaboration in the peripheral neuromuscular junction (NMJ) [8]. Here, we investigate the role of dFMRP in the central brain, focusing on the mushroom body (MB), the learning and memory center [9, 10]. In MB neurons, dFMRP bidirectionally regulates multiple levels of structural architecture, including process formation from the soma, dendritic elaboration, axonal branching, and synaptogenesis. *Drosophila fmr1* (*dfmr*) null mutant neurons display more complex architecture, including overgrowth, overbranching, and abnormal synapse formation. In contrast, dFMRP overexpression simplifies neuronal structure, causing undergrowth, underbranching, and loss of synapse differentiation. Studies of ultrastructural *dfmr* mutant neurons reveal enlarged and irregular synaptic boutons with dense accumulation of synaptic vesicles. Taken together, these data show that dFMRP is a potent negative regulator of neuronal architecture and synaptic differentiation in both peripheral and central nervous systems.

Results and Discussion

Mushroom Body Structure Is Largely Normal in *dfmr* Null Mutants

Both mammalian and *Drosophila* Fragile X Mental Retardation Protein (FMRP) is enriched in neuronal soma, undetectable in nuclei, and comprises only a small percentage of protein present in neuronal processes [11–14]. Similar to that found in the mushroom body (MB), dFMRP is prominently enriched in the soma of all neurons but is undetectable in nuclei (Figure 1A). The protein is present at high levels only within cell body cytoplasm, with little or no detectable dFMRP in dendrites or axonal projections. The mushroom body has four structural sections including cell bodies, dendrites (i.e., calyx), peduncle, and the axon lobes (Figure 1B). dFMRP is similarly expressed in the three classes of neurons; γ, α'/β', and α/β neurons [15]. γ neurons project a single horizontal axon, whereas α'/β' and α/β neurons have two axon projections, one horizontal and one vertical (Figure 1B). We took advantage of the relative simplicity of these neurons to analyze the role of dFMRP in their morphological differentiation. Here, we used the MARCM (*m*osaic *a*nalysis with *r*epressible *c*ell *m*arker) system [16], which uniquely labels single homozygous mutant neurons to reveal the whole projections of labeled neurons in the intact brain.

In FraX patients and *fmr1* knockout mice, brain morphology is grossly normal with no detectable abnormalities in specific brain regions [17, 18]. Similarly, null *dfmr* mutants display normal gross-brain morphology, including an architecturally normal mushroom body (Figure 1B, [19]). Mild overgrowth of the β lobe, resulting in the crossing of the brain midline, was observed in some mutants (see also [20]). In contrast, dFMRP overexpression (OE) caused dramatic structural defects in mushroom body axon lobes (Figure 1B), with the β lobe always overextended across the midline. The β' lobe often displayed apparently random directions of axon projection often outside of the mushroom body domain (Figure 1B). The γ lobe always displayed a dramatic decrease in volume and was even completely lost (Figure 1B). Thus, *dfmr* null mutants display only subtle defects in gross mushroom body architecture, whereas *dfmr* overexpression causes dramatic defects. Because FraX is caused by loss of FMRP, we therefore turned our attention to the single-cell and subcellular level to examine neuronal architecture.

Loss of dFMRP Converts Unipolar Neurons into Multipolar Neurons

The MARCM technique provides a uniquely powerful approach for examining mutant neurons in situ at a single cell level of resolution [16]. All the analyses presented in this study represent quantification from single, isolated *dfmr* mutant mushroom body neurons in an otherwise nonmutant brain. To make sure all phenotypes arose from *dfmr* mutation, we used two independently generated *dfmr* null mutant alleles, which represent overlapping intragenic deficiencies (Figure 2A), $dfmr^{50M}$ [8] and $dfmr^{3}$ [19]. In addition, dFMRP was overexpressed in single neurons to examine the consequence of excess protein. For controls, single-cell clones of GFP-expressing wild-type (WT) neurons were made (Figure 2B). In turn, we examined each region of the mutant neurons, progressing from the cell body through the dendrites, axons, and synapses.

Mushroom body neurons are exclusively unipolar [15, 21]. Cell bodies extend only a single primary process, which subsequently branches to form distinctive dendrites and axon projection (Figure 2B). A small minority of wild-type cells display one to two tiny hair-like additional projections (arrow), but these processes are always very short and thin compared with the primary process. In wild-type, it is exceptionally rare for the

*Correspondence: kendal.broadie@vanderbilt.edu

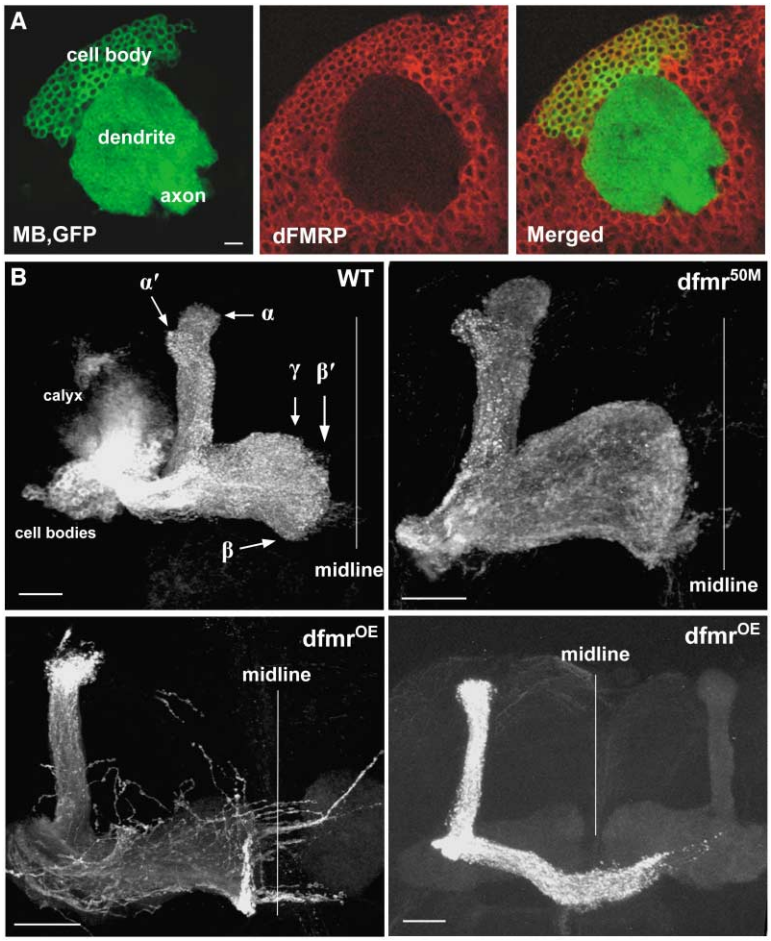

Figure 1. dFMRP Expression and Function in the Mushroom Body

(A) Mushroom body labeled by UAS-CD8-GFP (green) driven by GAL4-OK107. The cell bodies, dendrites, and axons are indicated. dFMRP expression (red) is predominantly present in soma, being undetectable in dendrites and axons. The scale bar represents 10 μm.

(B) Mushroom body morphology revealed by large MARCM clones, labeled by UAS-CD8-GFP, and driven by GAL4-OK107. Wild-type (WT) structure showing the labeled axon lobes [15]. Occasional axon extension beyond the β lobe is observed. *dfmr* null mutants display grossly normal structure. Mild β lobe overgrowth is observed at a slightly higher frequency than wild-type. dFMRP overexpression (*dfmr*^{OE}) caused a high frequency of apparently random growth of all axon lobes. Especially in β lobe, dramatic overgrowth was observed at high frequency. All scale bars represent 25 μm.

additional processes to contain any branches or elaborations. In contrast, *dfmr* mutant neurons have a strong tendency to extend supernumerary processes, thus always converting the characteristic unipolar neurons in wild-type into multipolar neurons in mutants (Figure 2B). In addition, the additional processes in *dfmr* mutants are usually long and thick, branch extensively and differentiate varicosities characteristic of synapses (Figure 2B). In contrast, dFMRP overexpression results in even fewer processes than wild-type, generating an entirely smooth cell body profile. We quantified the average number of additional processes in single α′/β′ neurons. Null mutants display a 3-fold increase in the number of cell body processes (WT, 1.27 ± 0.3 n = 11; *dfmr*^{50M}, 3.84 ± 0.53, n = 19; *dfmr*^{3}, 3.75 ± 0.72, n = 12), whereas dFMRP overexpression reduces the number of processes 2-fold (WT, 1.27 ± 0.3; *dfmr*^{OE}, 0.64 ± 0.2, n = 22; Figure 2C). Similar phenotypes were also observed in γ and α/β neurons. These data show that dFMRP strongly negatively regulates the generation of processes from neuronal cell bodies.

dFMRP Negatively Regulates Dendritic Elaboration

Several common features of mushroom body neuron dendritic arbors aid in the description of *dfmr* mutant phenotypes. First, all three classes of neurons have three to four primary dendritic branches. Second, primary branches rarely contain higher-order branches along their initial length. Third, primary branches end with a fine dendritic terminal arbor that forms a highly characteristic "claw-like" structure (Figure 3; [22]). We used these conserved features as a basis to analyze the role of dFMRP in dendrite morphogenesis. Late-born α/β neurons (mitotic recombination was induced >12 hr after pupa formation; [22]) were used for detail morphometric studies.

Dendrites on *dfmr* mutant neurons are consistently abnormal in morphology and projection, owing to the increased complexity of several structural features (Figure 3). The number of primary dendritic branches are more variable in the mutant, ranging from two to six (compared to three to four in wild-type). In addition, nearly all mutant dendrite processes have clear supernumerary higher-order branches, and the clustered, fine dendritic arbors normally restricted to the extreme termini (the claw-like structure; [22]) spread aberrantly along the entire length of mutant dendritic branches (Figure 3). These excess fine dendritic processes convert the clear, orderly wild-type dendrites into disordered, "cotton wool-like" dendrites in *dfmr* mutants. On the other hand, dFMRP-overexpressing mutants lose the clustered fine dendritic arbors and show severe reduction or complete loss of the claw-like structure at the terminal of dendritic branches (Figure 3). Thus, removal of dFMRP increases the branching and structural complexity of dendritic processes, whereas overexpres-

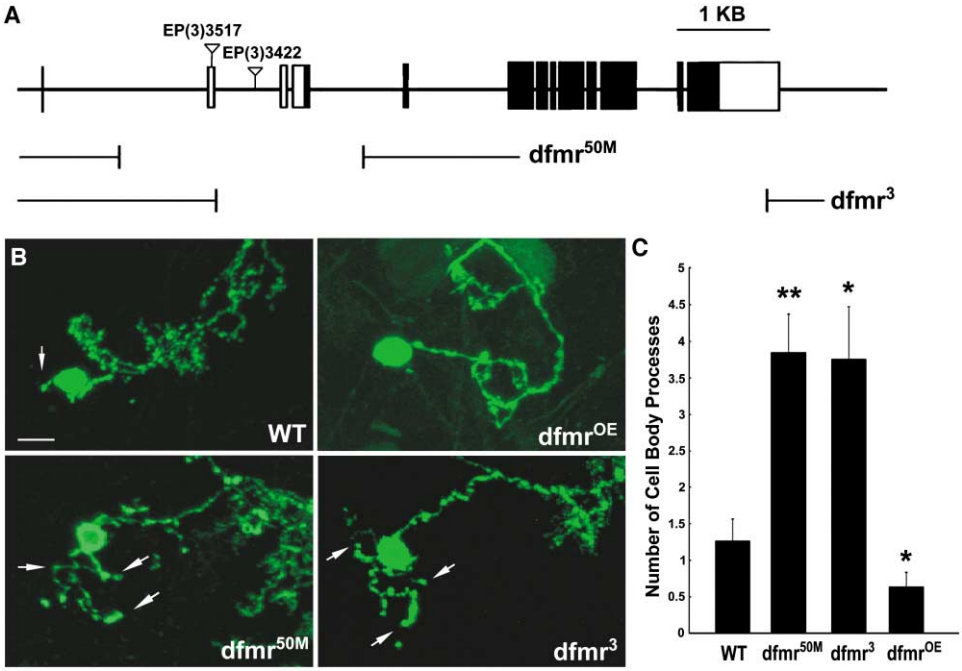

Figure 2. dFMRP Loss of Function Results in Aberrant Multipolar Neurons

(A) Genomic structure of the *dfmr* locus and the two independent *dfmr* intragenic deletion mutants used in this study; $dfmr^{50M}$ [8] and $dfmr^{3}$ [19]. Note that the $dfmr^{3}$ deletion reported here has verified breakpoints that differ from what was reported in Dockendorff, et al.

(B) Representative images of α'/β' neuronal soma and processes in single-cell MARCM clones. Wild-type (WT) neurons are typically unipolar, but, with rare frequency, there are 1–2 other short processes (arrow). These tiny processes lack secondary branches. Overexpression of dFMRP (OE) results in a cleaner cell body, with no excess processes. In contrast, *dfmr* mutant neurons always display multiple processes (arrows), becoming characteristically multipolar. These supernumerary processes are multibranched and contain varicosities resembling synaptic boutons. The scale bar represents 5 μm.

(C) Quantification of the number of processes projecting from cell bodies. The bars show the mean ± SEM. Significance: $0.001 < p < 0.05$ (*); $0.0001 < p < 0.001$ (**).

sion of dFMRP decreases dendritic branching and simplifies the arbor. These data show that dFMRP functions as a negative regulator of dendritic elaboration.

dFMRP Negatively Regulates Axonal Branching

Progressing from the cell body and through the dendritic arbor, we next consider the role of dFMRP on axonal projection and structure. The initial focus was the γ neuron because it has only one axonal branch and a particularly simple elaborative pattern in the mushroom body. The wild-type γ axon enters the horizontal axon lobe from the ventral edge, bends upwards to enter the γ lobe, and terminates near the dorsal boundary of the horizontal lobe (Figure 4A). The wild-type γ neuron never branches prior to entering the γ lobe but typically has several specific small branches along the main process [15].

The axons of *dfmr* mutant γ neurons are much more structurally elaborate than those of wild-type. Mutant neurons always display significantly increased axonal branching and always have significantly more and longer axonal branches (Figure 4A). These large, supernumerary branches do not follow the main axon trajectory, but rather they extend in apparently random directions to invade inappropriate territory (Figure 4A). Some of the excess branches in mutants are so large that the γ neuron appears to possess duplicate main-axonal processes (Figure 4A). The number of these large branches (>5 μm in length) increased on average by $>50\%$ (WT, 3.74 ± 0.28, $n = 19$; $dfmr^{3}$, 6.46 ± 0.8, $n = 13$; $dfmr^{50M}$, 5.33 ± 0.33, $n = 21$; Figure 4B), and the total length of axon branches also significantly increased (WT, 65.68 ± 5.07 μm; $dfmr^{3}$, 103.33 ± 8.5 μm; $dfmr^{50M}$, 84.29 ± 5 μm; Figure 4C). In contrast, dFMRP overexpression caused underbranching and dramatically reduced growth (Figure 4A). Most dFMRP overexpression γ neurons maintain their process along the ventral edge of the horizontal lobe and aberrantly invade the β lobe. With excess dFMRP, the number of axonal branches was decreased by 65% (WT, 3.74 ± 0.28; $dfmr^{OE}$, 1.38 ± 0.26, $n = 24$; Figure 4B), and the total axonal branch length was decreased by 75% (WT, 65.68 ± 5.07 μm; $dfmr^{OE}$, 16.86 ± 3.8; Figure 4C). Thus, excess FMRP dramatically simplifies axonal projection and results in premature termination. Similar phenotypes were observed in the other two classes of neurons (α'/β', Figure 4D; and α/β, data not shown). These results demonstrate that dFMRP functions to negatively regulate axonal branching in mushroom body neurons, resulting in defective axonal guidance and connectivity.

dFMRP Regulates Synapse Differentiation

Loss of dFMRP results in striking defects in neuronal architecture (Figures 2–4), suggesting that synaptic connectivity might be impaired. Recent work in mouse *fmr1* mutants has indicated defects in synaptic plasticity [23]. Likewise, our previous work on *dfmr* mutants in the

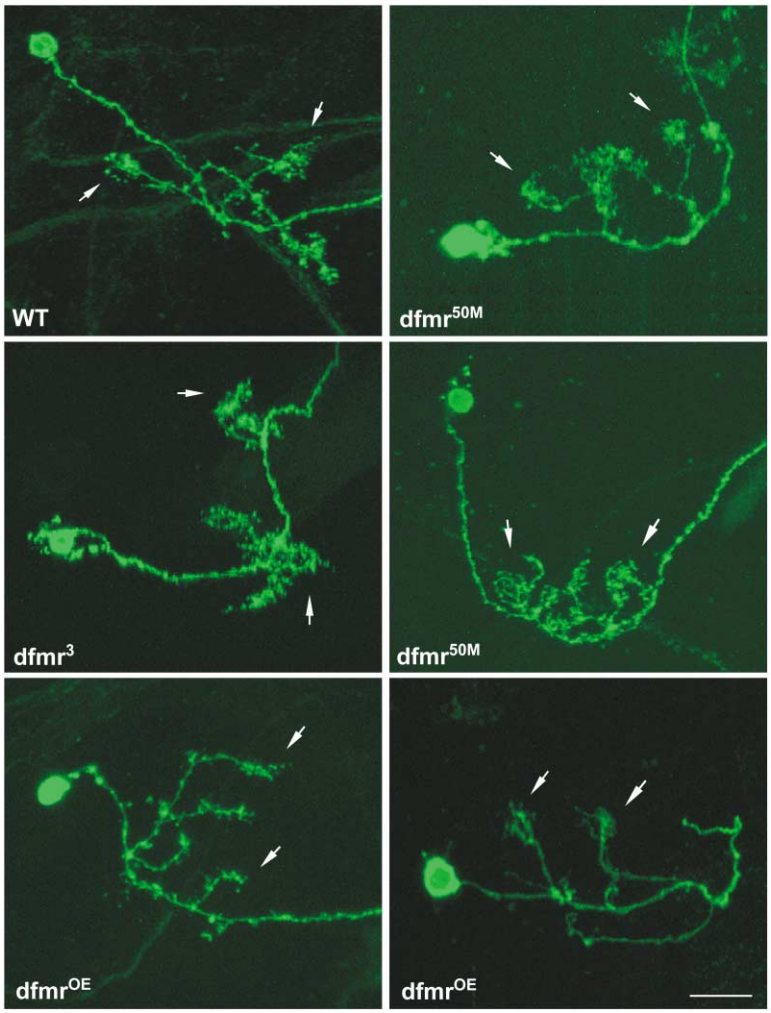

Figure 3. dFMRP Negatively Regulates Dendrite Elaboration

Representative images of late-born α/β neuron dendritic arbors in single-cell MARCM clones. Wild-type (WT) dendrites typically display three primary branches. There are no higher-order branches but only a single, well-defined claw-like structure of fine processes at the termini (arrows). Three images of *dfmr* mutant neurons show more complex and disordered dendritic structure. Primary dendrites display clear secondary branches. The fine dendritic processes, normally restricted to the termini, spread aberrantly along the primary branches. These defects convert the orderly wild-type dendrites into disordered, cotton wool-like structures. dFMRP overexpression results in loss of the claw-like termini. Arrows show the reduced or absent claw-like structures. The scale bar represents 10 μm.

Drosophila neuromuscular junction (NMJ) and eye has strongly suggested specific defects at the synapse [8]. Therefore, we next examined synaptic differentiation in *dfmr* mutant MB clones at both the light and electron microscopy levels.

In wild-type animals, mushroom body axonal processes display a relatively smooth profile, with only subtle varicosities indicative of synaptic connections [24]. In contrast, *dfmr* mutant axons show a markedly discontinuous profile, with enlarged varicosities fairly evenly distributed along axons, producing a highly characteristic "beads on a string" appearance (Figures 4A and 4D). In contrast, dFMRP overexpression resulted in a smoother axon profile than wild-type (Figures 4A and 4D). The position and spacing of these varicosities strongly suggests that they represent the altered features of presynaptic boutons.

To examine in detail synaptic differentiation in *dfmr* mutants, we next employed electron microscopy to examine MARCM mutant clones. For labeling, we used a peroxidase-conjugated anti-CD8 antibody followed by a Ni^{2+}-enhanced DAB reaction to produce an electron-dense, membrane-associated signal clearly marking the *dfmr* mutant neurons (Figure 5A and see Experimental Procedures). We focused our analysis on α′/β′ axons in the horizontal axon lobe (Figure 5B); they showed an extensive overbranching phenotype and prominently discontinuous axon profiles at the light microscope level.

The first objective was to confirm the light microscope impression of enlarged presynaptic bouton size. We therefore serial sectioned labeled α′/β′ axons and measured the cross-section area of all profiles containing T-bar active zones, which define presynaptic neurotransmitter release sites (Figures 5D and 5F, arrows). The average cross-section, bouton area of *dfmr* mutant neurons was significantly ($P=0.05$) enlarged compared to labeled wild-type neurons (WT, mean = 0.19 ± 0.01 μm^2, n = 97; *dfmr*^{50M}, mean = 0.24 ± 0.02, n = 108; Figures 5D and 5E). In addition, *dfmr* mutant boutons display a markedly more variable size. In the 200+ boutons measured, the largest and smallest bouton ranges both occurred in mutant neurons (Figure 5E); the area of the largest *dfmr* bouton was >50% larger than the largest wild-type bouton, and the area of smallest *dfmr* bouton was ~35% decreased compared to the smallest wild-type bouton. These results suggest that dFMRP negatively regulates the morphological differentiation of synaptic boutons, and also increases the fidelity of bouton size.

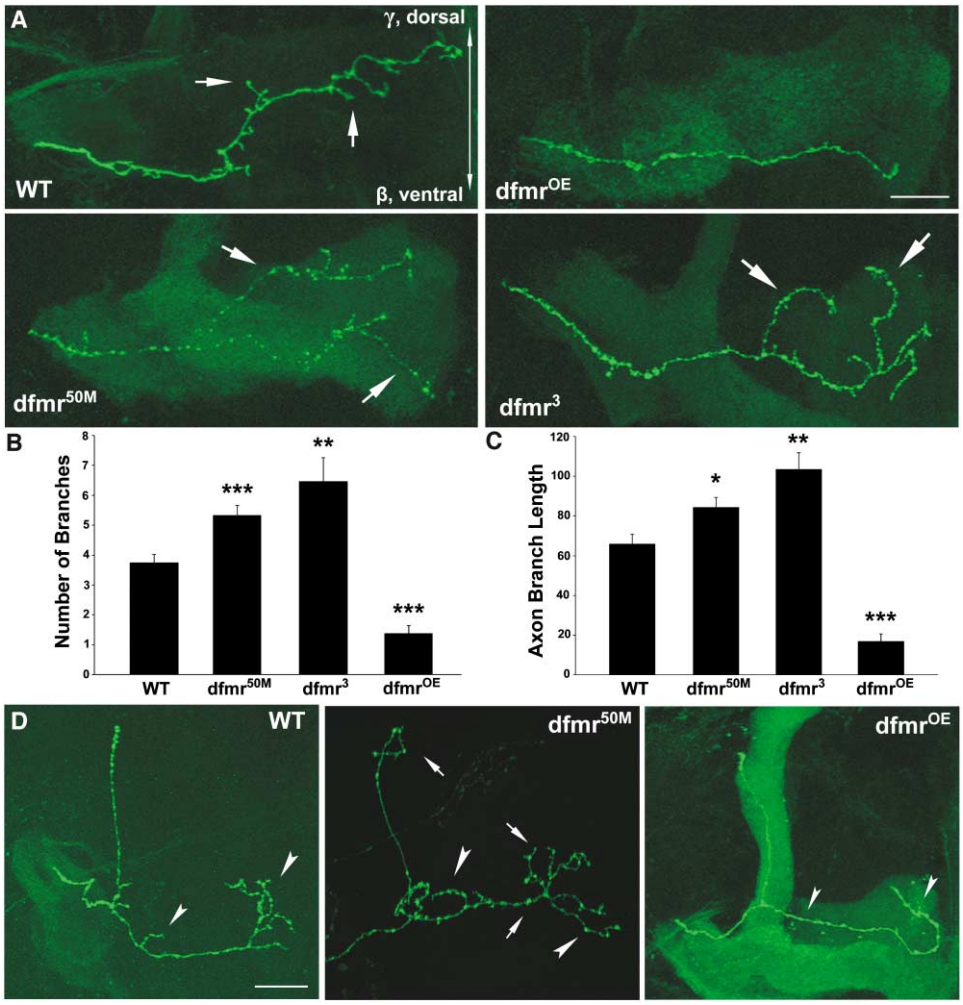

Figure 4. dFMRP Negatively Regulates Axonal Branching

(A) Representative γ neuron axons in single-cell MARCM clones. The γ neuron axon normally enters the horizontal axon lobe from the ventral edge, bends upwards to enter the γ lobe, and finally projects to the dorsal boundary of the horizontal lobe. In wild-type (WT) neurons, the axon projection has only one main axonal branch with some specific small branches (arrows) along the main process. dFMRP overexpression causes dramatic under-branching of the axon. The γ neurons maintain their processes along the ventral edge of the horizontal lobe and aberrantly invade the β lobe. The *dfmr* mutants display the opposite phenotype of axonal overbranching. Null mutant neurons always have more and longer axonal branches. These large branches don't follow the main axon direction but rather extend in an apparently random direction (arrows). The scale bar represents 10μm.

(B) Quantification of the large branches (>5 μm) for a single γ axon.

(C) Quantification of total branch length of a single γ axon. WT, n = 19; *dfmr*^{50M}, n = 21; *dfmr*^{3}, n = 13; OE, n = 24. Bars show mean ± SEM. Significance $0.001 < p < 0.05$ (*); $0.0001 < p < 0.001$ (**); $p < 0.0001$ (***).

(D) Representative α′/β′ neuron axon morphologies in single-cell MARCM clones. WT neurons characteristically have one small side branch in proximal quarter region and branches clustered at the terminal of the horizontal lobes (arrowheads). Note that GFP distribution is relatively even along the axon, with only small varicosities. *dfmr* mutant neuron axons display overbranching. Axons have longer side branches in the proximal quarter and terminal branching region. The GFP distribution is strikingly altered, with enlarged puncta (arrows) distributed along the axons. In the overexpression neuron, arrowheads indicate the positions of branches in the WT axon. The scale bar represents 20 μm.

The immediately striking observation was that *dfmr* mutant presynaptic boutons were almost filled with evenly sized, electron-lucent synaptic vesicles, clearly several orders of magnitude more vesicles than in control boutons (Figures 5C, 5D, and 5F). Indeed, vesicle density within mutant boutons was so high that it often precluded the ability to resolve other features of the active zone and effectively prevented any ability to clearly resolve individual vesicles for quantification. Therefore, to partially quantify the vesicle accumulation phenotype, we measured the bouton area fully occupied by vesicles as a percentage of the total bouton area (Figure 5G). In control neurons, slightly less than 50% of the bouton area is normally occupied by synaptic vesicles, whereas nearly 75% of the bouton is occupied by vesicles in *dfmr* mutant neurons. Thus, the average area occupied by vesicles is increased 50% ($p < 0.001$) in *dfmr* boutons compared to internal control boutons (WT, mean = 49% ± 3%, n = 27; *dfmr*^{50M} mean = 73% ± 5%, n = 25; Figures 5F and 5G). In fact, the actual vesicle

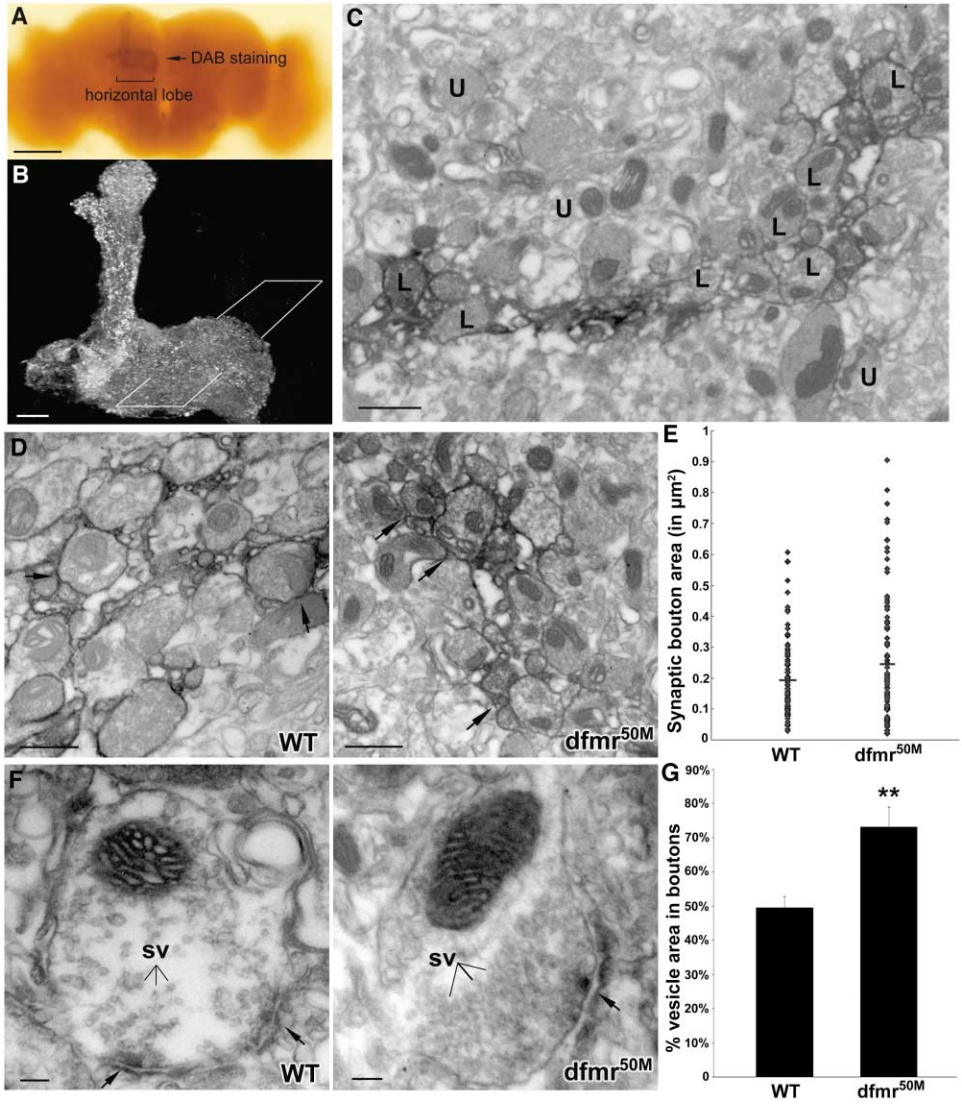

Figure 5. dFMRP Regulates Synaptic Differentiation

(A) DAB-stained brain revealing a large MARCM clone within the mushroom body. The scale bar represents 100 μm.

(B) Confocal image of the whole mushroom body MARCM clone. Quadrangle represents the plane of section through the horizontal lobe, where all electron micrographs were taken. The scale bar represents 10 μm.

(C) Electron micrograph (11500×) of the mushroom body horizontal lobe; labeled MARCM clone cells (L) and unlabeled cells (U). The scale bar represents 500 nm.

(D) Electron micrograph (25000×) of a mushroom body horizontal lobe with wild-type (WT, left) and *dfmr*^{50M} (right) MARCM clones. Arrows indicate the electron-dense, labeled bouton membrane. The scale bar represents 500 nm.

(E) Quantification of labeled bouton area in both WT and *dfmr*^{50M} clones. The *dfmr* null mutant neurons display a significantly enlarged average bouton area and more variable distribution of bouton sizes than wild-type (WT, n = 97; *dfmr*^{50M}, n = 108, p = 0.05).

(F) High magnification of a single synaptic bouton from WT (left) and *dfmr*^{50M} null mutant (right) neurons. The null mutant boutons show a dramatically increased density of synaptic vesicles (SV) throughout the bouton interior and at presynaptic active zones (arrows). The scale bar represents 100 nm.

(G) Quantification of synaptic vesicle density. Bars indicate the percentage of the total bouton area occupied by synaptic vesicles. (WT, n = 25; *dfmr*^{50M}, n = 27, p < 0.001).

accumulation in mutant boutons is much greater than is reflected in these numbers because vesicles in the mutant are much more densely accumulated to the extent that normally prevents clear resolution of individual vesicles. A vesicle accumulation defect of this severity has not been previously reported for *Drosophila*. This defect could be due to hyperactive vesicle biogenesis or an arrest in vesicular exocytosis, either one resulting in increased vesicle density. Our previous studies have revealed synaptic vesicle accumulation only in mutants with severely impaired vesicular exocytosis and neurotransmitter release, such as *dUNC-13* and *dCAPs* mutants [25, 26]. Thus, *dfmr* mutant synapses of mushroom body neurons display aberrant ultrastructural profiles

consistent with defective synaptic function and impaired neurotransmitter release.

Conclusions

Here, we examined the role of dFMRP in the structural differentiation of the three neuronal classes (γ, α'/β', and α/β neurons) comprising the mushroom body, the insect brain's learning and memory center suggested to functionally correspond to the mammalian hippocampus [9, 10, 27]. In all neuronal classes, loss of dFMRP causes increased structural complexity throughout the entire neuron, including the extension of additional processes from neuronal soma, overbranching and overgrowth of both the dendritic field and axon processes, and consequent defects in projection. Correspondingly, dFMRP overexpression causes decreased structural complexity throughout the entire neuron, including reduction of cell body processes, undergrowth of dendritic arbors, underbranching and undergrowth of axonal processes, and consequent defects in connectivity. Thus, the level of dFMRP bidirectionally regulates growth and architectural elaboration throughout these neurons, altering the availability of both synaptic input and output sites. Ultrastructure analysis of *dfmr* mutants shows enlarged synaptic boutons, irregular bouton size, and abnormal synaptic vesicle accumulation. These defects indicate impaired synaptogenesis and suggest arrested synaptic function, including either abnormal vesicle biogenesis or impaired synaptic vesicle exocytosis and consequent loss of neurotransmitter release.

In mammals, FMRP has been clearly implicated in synaptic mechanisms, although with a predominantly postsynaptic association. FMRP mRNA and protein are both found localized in dendritic spines in the mouse brain [13, 28], and FMRP is locally translated in an activity-dependent mechanism that requires activation of metabotropic glutamate receptors [29, 30]. FMRP is, in turn, required for mGluR-dependent translation [29, 31]. Mouse *fmr1* mutants have reduced GluR1 subunits at cortical synapses but not in the hippocampus or cerebellum, and similarly, long-term potentiation is reduced in the cortex but not in the hippocampus [32]. Huber et al. [23] showed that FMRP is also required for mGluR-dependent long-term depression in the hippocampus. Although these results suggest primarily postsynaptic roles for FMRP, identification of FMRP mRNA targets has conversely suggested mostly presynaptic functions. Among presynaptic targets identified, there have been MUNC-13, NAP-22, SEC-7, and RAB-5 [1, 33]. These putative FMRP targets provide possible mechanistic explanations for the presynaptic defects in *Drosophila* reported here and previously [8].

Experimental Procedures

Genetics

The following *Drosophila* strains were generated by standard genetic methods: (1) *heatshock-FLP, mouse CD8-GFP; FRT82B, tubulin P-GAL80/TM3; GAL4-OK107*. (2) *y, w; FRT82B/TM3*. (3) *FRT82B, dfmr^{50M}/TM6*. (4) *FRT82B, dfmr^{3}/TM6*. (5) *FRT82B, UAS-dfmr*. *GAL4-OK107* was used as the driver to visualize mushroom body clones in all cases [34]. *Mouse CD8-GFP* was used to label clones. All *dfmr^{50M}*, *dfmr^{3}*, and *UAS-dfmr* insertions were recombined to the *FRT82B* chromosome by standard methods, based on the presence of *FRT82B* carrying the G418 resistance [35] and PCR confirmation of all the genetic elements.

Immunohistochemistry

The following antibodies were used: rat anti-mouse CD8a, 1:100 (Caltag); mouse anti-*Drosophila* Fasciclin II, 1:10 (Developmental Studies Hybridoma Bank); mouse anti-dFMRP, 1:1000 (Developmental Studies Hybridoma Bank); FITC-conjugated goat anti-rat IgG, 1:100 (Jackson); goat Cy3-conjugated goat anti-mouse IgG, 1:100 (Jackson); rat anti-*Drosophila* DLG, 1:100 (V. Budnik). All fluorescent images were collected using a ZEISS LSM510 META Laser Scanning Microscope and image collection software. All image processing was done with Adobe Photoshop 7.0.

Mosaic Analysis with a Repressible Cell Maker (MARCM)

The MARCM technique was employed as described in Lee and Luo [16]. To generate MARCM clones in the γ-neuron, embryos were collected within a 5 hr window and cultured at 25°C. Twenty-hour-old embryos were heat shocked at 37°C for 1 hr. To generate α'/β' and α/β MARCM clones, the same heat shock was done to 5-day-old larvae and 8-day-old pupa, respectively. Adult brains were dissected in 1× PBS, fixed in 4% paraformaldehyde for 30 min, and processed with immunostaining.

Morphological Quantification

All quantification was done on single-cell MARCM clones. For γ-neuron axonal quantification, the primary axon branch was identified first, and all other processes extended from this main trunk were counted as branches. The length of each branch was measured based on 3D images from confocal microscopy. All branch lengths of single-axon branches were added together to get the total cumulative length. For α'/β'-neuron cell body process quantification, all processes except the main process were counted. One branch was counted as one process. In mutants, branch numbers >10 (always difficult to tell apart) were counted as 10.

Electron Microscopy

Ultrastructural analyses of *Drosophila* brains were done with standard protocols [36, 37]. Briefly, 1–3-day-old adult brains with MARCM clones were dissected in 1× PBS buffer and immediately fixed for 30 min in 2% paraformaldehyde. The samples were subsequently rinsed with PBS-BSA buffer for 3 hr at 4°C, stained with rat anti-mouse CD8 antibody (1:100) for 12 hr at 4°C, washed with PBS horse serum buffer for 3 hr at 4°C, stained with biotinylated anti-rat IgG (1:50) for 12 hr at 4°C, and washed overnight in 1× PBS at 4°C. Brains were sequentially treated with Vectastain ABC kit (Vector Laboratories), stained with a Vector peroxidase substrate DAB kit, washed with PBS for 3 hr at 4°C, and incubated overnight in 1% glutaraldehyde at 4°C. Samples were transferred to 2% glutaraldehyde for 45 min, transferred to 1% osmium tetroxide in ddH_2O for 1 hr, and stained en bloc in 2% aqueous uranyl acetate for 1 hr. Brains were dehydrated and embedded in araldite. Ribbons of thin (~50 nm) sections were obtained with a Leica Ultracut UCT 54 Ultramicrotome and examined on a Phillips CM 12 TEM.

Ultrastructural Quantification

To assay bouton area, 25,000× images were used for comparing wild-type and *dfmr* mutant MARCM mushroom body clones. Areas were measured with National Institutes of Health (NIH) ImageJ software. To assay synaptic vesicle density, 25000× images were used. In *dfmr* mutant MARCM mushroom body clones, 2 μm circles were centered over the labeled cell and assays made of labeled bouton (*dfmr* mutant) and unlabeled boutons (control) in a nearest-neighbor comparison. Total bouton area and synaptic vesicle-occupied bouton area were measured with NIH ImageJ software.

Acknowledgments

We are most particularly grateful to R. Watts and J. Wang for advice on the MARCM technique and to L. Luo and T. Lee for kindly providing essential MARCM stocks. We thank T. Jongens and T. Dockendorff for providing *dfmr^{3}* mutant stocks. We thank the Vanderbilt Electron Microscopy Core Lab. We thank the members of the Broa-

die lab for insightful discussions and comments on the manuscript. This work was supported by a NIH grant HD40654 to K.B.

Received: June 4, 2004
Revised: August 31, 2004
Accepted: August 31, 2004
Published: October 26, 2004

References

1. Brown, V., Jin, P., Ceman, S., Darnell, J.C., O'Donnell, W.T., Tenenbaum, S.A., Jin, X., Feng, Y., Wilkinson, K.D., Keene, J.D., et al. (2001). Microarray identification of FMRP-associated brain mRNAs and altered mRNA translational profiles in fragile X syndrome. Cell *107*, 477–487.
2. Jin, P., and Warren, S.T. (2000). Understanding the molecular basis of fragile X syndrome. Hum. Mol. Genet. *9*, 901–908.
3. Li, Z., Zhang, Y., Ku, L., Wilkinson, K.D., Warren, S.T., and Feng, Y. (2001). The fragile X mental retardation protein inhibits translation via interacting with mRNA. Nucleic Acids Res. *29*, 2276–2283.
4. Schaeffer, C., Bardoni, B., Mandel, J.L., Ehresmann, B., Ehresmann, C., and Moine, H. (2001). The fragile X mental retardation protein binds specifically to its mRNA via a purine quartet motif. EMBO J. *20*, 4803–4813.
5. Hinton, V.J., Brown, W.T., Wisniewski, K., and Rudelli, R.D. (1991). Analysis of neocortex in three males with the fragile X syndrome. Am. J. Med. Genet. *41*, 289–294.
6. Irwin, S.A., Idupulapati, M., Gilbert, M.E., Harris, J.B., Chakravarti, A.B., Rogers, E.J., Crisostomo, R.A., Larsen, B.P., Mehta, A., Alcantara, C.J., et al. (2002). Dendritic spine and dendritic field characteristics of layer V pyramidal neurons in the visual cortex of fragile-X knockout mice. Am. J. Med. Genet. *111*, 140–146.
7. Nimchinsky, E.A., Oberlander, A.M., and Svoboda, K. (2001). Abnormal development of dendritic spines in FMR1 knock-out mice. J. Neurosci. *21*, 5139–5146.
8. Zhang, Y.Q., Bailey, A.M., Matthies, H.J., Renden, R.B., Smith, M.A., Speese, S.D., Rubin, G.M., and Broadie, K. (2001). *Drosophila* fragile X-related gene regulates the MAP1B homolog Futsch to control synaptic structure and function. Cell *107*, 591–603.
9. Davis, R.L. (1993). Mushroom bodies and *Drosophila* learning. Neuron *11*, 1–14.
10. Heisenberg, M. (2003). Mushroom body memoir: From maps to models. Nat. Rev. Neurosci. *4*, 266–275.
11. Devys, D., Lutz, Y., Rouyer, N., Bellocq, J.P., and Mandel, J.L. (1993). The FMR-1 protein is cytoplasmic, most abundant in neurons and appears normal in carriers of a fragile X premutation. Nat. Genet. *4*, 335–340.
12. Morales, J., Hiesinger, P.R., Schroeder, A.J., Kume, K., Verstreken, P., Jackson, F.R., Nelson, D.L., and Hassan, B.A. (2002). *Drosophila* fragile X protein, DFXR, regulates neuronal morphology and function in the brain. Neuron *34*, 961–972.
13. Weiler, I.J., Irwin, S.A., Klintsova, A.Y., Spencer, C.M., Brazelton, A.D., Miyashiro, K., Comery, T.A., Patel, B., Eberwine, J., and Greenough, W.T. (1997). Fragile X mental retardation protein is translated near synapses in response to neurotransmitter activation. Proc. Natl. Acad. Sci. USA *94*, 5395–5400.
14. Verheij, C., Bakker, C.E., de Graaff, E., Keulemans, J., Willemsen, R., Verkerk, A.J., Galjaard, H., Reuser, A.J., Hoogeveen, A.T., and Oostra, B.A. (1993). Characterization and localization of the FMR-1 gene product associated with fragile X syndrome. Nature *363*, 722–724.
15. Lee, T., Lee, A., and Luo, L. (1999). Development of the Drosophila mushroom bodies: Sequential generation of three distinct types of neurons from a neuroblast. Development *126*, 4065–4076.
16. Lee, T., and Luo, L. (1999). Mosaic analysis with a repressible cell marker for studies of gene function in neuronal morphogenesis. Neuron *22*, 451–461.
17. Bakker, C.E.e.a. (1994). Fmr1 knockout mice: A model to study fragile X mental retardation. The Dutch-Belgian Fragile X Consortium. Cell *78*, 23–33.
18. Reyniers, E., Martin, J.J., Cras, P., Van Marck, E., Handig, I., Jorens, H.Z., Oostra, B.A., Kooy, R.F., and Willems, P.J. (1999). Postmortem examination of two fragile X brothers with an FMR1 full mutation. Am. J. Med. Genet. *84*, 245–249.
19. Dockendorff, T.C., Su, H.S., McBride, S.M., Yang, Z., Choi, C.H., Siwicki, K.K., Sehgal, A., and Jongens, T.A. (2002). *Drosophila* lacking dfmr1 activity show defects in circadian output and fail to maintain courtship interest. Neuron *34*, 973–984.
20. Michel, C.I., Kraft, R., and Restifo, L.L. (2004). Defective neuronal development in the mushroom bodies of Drosophila fragile X mental retardation 1 mutants. J. Neurosci. *24*, 5798–5809.
21. Crittenden, J.R., Skoulakis, E.M., Han, K.A., Kalderon, D., and Davis, R.L. (1998). Tripartite mushroom body architecture revealed by antigenic markers. Learn. Mem. *5*, 38–51.
22. Zhu, S., Chiang, A.S., and Lee, T. (2003). Development of the Drosophila mushroom bodies: Elaboration, remodeling and spatial organization of dendrites in the calyx. Development *130*, 2603–2610.
23. Huber, K.M., Gallagher, S.M., Warren, S.T., and Bear, M.F. (2002). Altered synaptic plasticity in a mouse model of fragile X mental retardation. Proc. Natl. Acad. Sci. USA *99*, 7746–7750.
24. Watts, R.J., Schuldiner, O., Perrino, J., Larsen, C., and Luo, L. (2004). Glia engulf degenerating axons during developmental axon pruning. Curr. Biol. *14*, 678–684.
25. Aravamudan, B., Fergestad, T., Davis, W.S., Rodesch, C.K., and Broadie, K. (1999). Drosophila UNC-13 is essential for synaptic transmission. Nat. Neurosci. *2*, 965–971.
26. Renden, R., Berwin, B., Davis, W., Ann, K., Chin, C.T., Kreber, R., Ganetzky, B., Martin, T.F., and Broadie, K. (2001). *Drosophila* CAPS is an essential gene that regulates dense-core vesicle release and synaptic vesicle fusion. Neuron *31*, 421–437.
27. Zars, T. (2000). Behavioral functions of the insect mushroom bodies. Curr. Opin. Neurobiol. *10*, 790–795.
28. Antar, L.N., Afroz, R., Dictenberg, J.B., Carroll, R.C., and Bassell, G.J. (2004). Metabotropic glutamate receptor activation regulates fragile x mental retardation protein and FMR1 mRNA localization differentially in dendrites and at synapses. J. Neurosci. *24*, 2648–2655.
29. Todd, P.K., Mack, K.J., and Malter, J.S. (2003). The fragile X mental retardation protein is required for type-I metabotropic glutamate receptor-dependent translation of PSD-95. Proc. Natl. Acad. Sci. USA *100*, 14374–14378.
30. Weiler, I.J., and Greenough, W.T. (1999). Synaptic synthesis of the Fragile X protein: Possible involvement in synapse maturation and elimination. Am. J. Med. Genet. *83*, 248–252.
31. Greenough, W.T., Klintsova, A.Y., Irwin, S.A., Galvez, R., Bates, K.E., and Weiler, I.J. (2001). Synaptic regulation of protein synthesis and the fragile X protein. Proc. Natl. Acad. Sci. USA *98*, 7101–7106.
32. Li, J., Pelletier, M.R., Perez Velazquez, J.L., and Carlen, P.L. (2002). Reduced cortical synaptic plasticity and GluR1 expression associated with fragile X mental retardation protein deficiency. Mol. Cell. Neurosci. *19*, 138–151.
33. Miyashiro, K.Y., Beckel-Mitchener, A., Purk, T.P., Becker, K.G., Barret, T., Liu, L., Carbonetto, S., Weiler, I.J., Greenough, W.T., and Eberwine, J. (2003). RNA cargoes associating with FMRP reveal deficits in cellular functioning in Fmr1 null mice. Neuron *37*, 417–431.
34. Connolly, J.B., Roberts, I.J., Armstrong, J.D., Kaiser, K., Forte, M., Tully, T., and O'Kane, C.J. (1996). Associative learning disrupted by impaired Gs signaling in Drosophila mushroom bodies. Science *274*, 2104–2107.
35. Xu, T., and Rubin, G.M. (1993). Analysis of genetic mosaics in developing and adult Drosophila tissues. Development *117*, 1223–1237.
36. Barth, M., Hirsch, H.V., Meinertzhagen, I.A., and Heisenberg, M. (1997). Experience-dependent developmental plasticity in the optic lobe of Drosophila melanogaster. J. Neurosci. *17*, 1493–1504.
37. Yasuyama, K., Meinertzhagen, I.A., and Schurmann, F.W. (2002). Synaptic organization of the mushroom body calyx in Drosophila melanogaster. J. Comp. Neurol. *445*, 211–226.